

MHD Micropolar Fluid Flow Toward a Stagnation Point On a Vertical Surface Under Induced Magnetic Field With Radiative Heat Flux

A. Adhikari

Assistant Professor of Mathematics
Shyampur Siddheswari Mahavidyalaya
P.O.-Ajodhya, Howrah-711312, W.B., INDIA

Abstract:

In this paper, a steady two-dimensional Magnetohydrodynamic (MHD) mixed convection stagnation point flow of an incompressible, viscous and electrically conducting micropolar fluid toward a stretching/shrinking vertical surface with prescribed surface heat flux is investigated. The effects of induced magnetic field and the radiative heat flux are taken into account. The transformed differential equations are solved numerically by a finite-difference scheme, known as Keller-box method. The results for skin friction, heat transfer and induced magnetic field coefficients are obtained. The velocity, microrotation and temperature distribution for various parameters are shown graphically. The present results are compared with existing results in literature and establish to be in good conformity.

Key words: micropolar fluid, stagnation point, stretching/shrinking sheet, radiative heat flux, induced magnetic field.

AMS subject classification: 76W05, 76S05

1. Introduction

The theory of microrotation fluids, first studied by Eringen (1966), displays the effects of local rotary inertia and couple stresses, can explain the flow behavior due to the microscopic effects arising from the local structure and micromotions of the fluid elements in which the classical Newtonian

fluids theory is inadequate. The behaviors of non-Newtonian fluids such as polymeric fluids, liquid crystals, paints, animal blood, colloidal fluids, ferro-liquids etc. can be described with the help of a mathematical model using this theory. Several researchers have investigated the theory and its applications such as Ariman et al. (1973, 1974), Lukaszewick (1999), Eringen (2001), Ishak et al. (2007, 2008) etc.

The stagnation point flow is important in many practical applications such as cooling of nuclear reactors, cooling of electronic devices, extrusion of plastic sheets, paper production, glass blowing, metal spinning and drawing plastic films and many hydrodynamic processes. Laminar mixed convection in two-dimensional stagnation flows around heated surfaces in the case of arbitrary surface temperature and heat flux variations was examined by Ramachandran et al. (1988). They established a reverse flow developed in the buoyancy opposing flow region and dual solutions are found to exist for a certain range of the buoyancy parameter. Devi et al. (1991) extended this work for unsteady case. Lok et al. (2005) studied the case for a vertical surface immersed in a micropolar fluid. Chin et al. (2007), Ling et al. (2007) and Ishak et al.

(2007, 2008) reported the existence of dual solutions in the opposing flow case.

The study of the boundary layer flow under the influence of a magnetic field with the induced magnetic field was considered by few authors. Raptis and Perdikis (1984) studied the MHD free convection boundary layer flow past an infinite vertical porous plate. Later, Kumari et al. (1990) considered prescribed wall temperature or heat flux, and Takhar et al. (1993) studied the time dependence of a free convection flow. Ali et al. (2011) discussed MHD mixed convection boundary layer flow under the effect of induced magnetic field. Hydromagnetic thermal boundary layer flow of a perfectly conducting fluid was observed by Das (2011). Mukhopadhyay et al. (2012) discussed Lie group analysis of MHD boundary layer slip flow past a heated stretching sheet in presence of heat source/sink. Shit and Halder (2012) examined thermal radiation effects on MHD viscoelastic fluid flow over a stretching sheet with variable viscosity. Heat transfer effects on MHD viscous flow over a stretching sheet with prescribed surface heat flux was studied by Adhikari and Sanyal (2013).

In this paper, a steady MHD mixed convection stagnation point flow of an incompressible micropolar fluid towards a stretching/shrinking vertical surface with prescribed surface heat flux is studied. The effects of induced magnetic field and the radiative heat flux are taken into account.

2. Mathematical Formulation

Consider a steady two-dimensional MHD flow of an incompressible electrically conducting micropolar fluid near the stagnation point on a vertical plate with prescribed surface heat flux with a velocity proportional to the distance from the fixed

origin O of a stationary frame of reference (x,y) , as shown in figure 1. A uniform induced magnetic field of strength H_0 is assumed to be applied in the positive y -direction, normal to the vertical plate. The normal component of the induced magnetic field H_2 vanishes when it reaches the wall and the parallel component H_1 approaches the value of H_0 . It is assumed that the velocity of the flow external to the boundary layer $U(=ax)$ and the surface heat flux $q_w(=bx)$ of the plate are proportional to the distance x from the stagnation point, where a, b are constants.

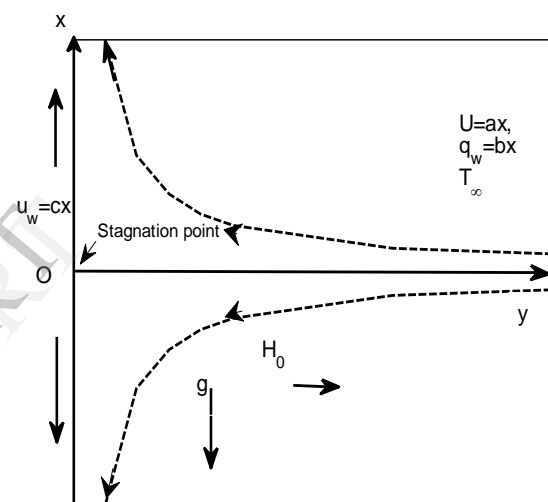


Fig 1: Sketch of the Problem

The magnetic Reynolds number of the flow is taken to be large enough so that the induced magnetic field is not negligible. Under the Boussinesq and the boundary layer approximations the governing equations are given by

$$\frac{\partial u}{\partial x} + \frac{\partial v}{\partial y} = 0, \quad (1)$$

$$\frac{\partial H_1}{\partial x} + \frac{\partial H_2}{\partial y} = 0, \quad (2)$$

$$u \frac{\partial u}{\partial x} + v \frac{\partial u}{\partial y} = U \frac{dU}{dx} + \left(\frac{\mu + \kappa}{\rho} \right) \frac{\partial^2 u}{\partial y^2} + \frac{\kappa}{\rho} \frac{\partial N}{\partial y} + \frac{\mu_0}{\rho} \left(H_1 \frac{\partial H_1}{\partial x} + H_2 \frac{\partial H_1}{\partial y} \right)$$

$$-\frac{\mu_0}{\rho} H_e \frac{\partial H_e}{\partial x} + g\beta(T - T_\infty), \quad (3)$$

$$u \frac{\partial H_1}{\partial x} + v \frac{\partial H_1}{\partial y} - H_1 \frac{\partial u}{\partial x}$$

$$-H_2 \frac{\partial u}{\partial y} = \alpha_1 \frac{\partial^2 H_1}{\partial y^2}, \quad (4)$$

$$\rho j \left(u \frac{\partial N}{\partial x} + v \frac{\partial N}{\partial y} \right) = \gamma \frac{\partial^2 N}{\partial y^2} - \kappa \left(2N + \frac{\partial u}{\partial y} \right), \quad (5)$$

$$u \frac{\partial T}{\partial x} + v \frac{\partial T}{\partial y} = \alpha \frac{\partial^2 T}{\partial y^2} - \frac{1}{\rho c_p} \frac{\partial q_r}{\partial y}, \quad (6)$$

Subject to the boundary conditions

$$\text{at } y = 0: u = u_w(x) = cx, \\ v = v_w(x), N = -n \frac{\partial u}{\partial y},$$

$$\frac{\partial T}{\partial y} = -\frac{q_w}{k}, \frac{\partial H_1}{\partial y} = H_2 = 0, \quad (7)$$

$$\text{at } y \rightarrow \infty: u \rightarrow u_e(x) = ax, \\ N \rightarrow 0, T \rightarrow T_\infty,$$

$$H_1 = H_e(x) = H_0 \frac{ax}{\nu}. \quad (8)$$

where u and v are the velocity components along the x and y -axis respectively, $u_w(x)$ the wall shrinking or stretching velocity ($c > 0$ for stretching, $c < 0$ for shrinking and $c = 0$ for static wall), $v_w(x)$ the wall mass flux velocity, N is the microrotation or angular velocity whose direction of rotation is in the xy plane, μ is the dynamic viscosity, μ_0 is the magnetic permeability, ρ is the density of the fluid, j is the micro-inertia per unit mass, i.e., micro-inertia density, γ is the spin gradient viscosity, κ is the vortex viscosity or micro-rotation viscosity, T is the fluid temperature in the boundary layer, β is the thermal expansion coefficient, α is the

thermal diffusivity, α_1 is the magnetic diffusivity, k is the thermal conductivity, q_w is the wall heat flux. Note that n is a constant such that $0 \leq n \leq 1$. When $n = 0$ then $N = 0$ at the wall represents concentrated particle flows in which the microelements close to the wall surface are unable to rotate. This case is also known as the strong concentration of microelements. When $n = 1/2$, we have the vanishing of anti-symmetric part of the stress tensor and denotes weak concentration of microelements, the case $n = 1$ is used for the modeling of turbulent boundary layer flows. We shall consider here both cases of $n = 0$ and $n = 1/2$. Assume $\gamma = \left(\mu + \frac{\kappa}{2} \right) j = \mu \left(1 + \frac{K}{2} \right) j$, where $K = \frac{\kappa}{\mu}$ is the material parameter. This assumption is invoked to allow the field of equations that predicts the correct behavior in the limiting case when the microstructure effects become negligible and the total spin N reduces to the angular velocity [Ahmadi (1976), Yuce(1989)].

By using the Rosseland approximation the radiative heat flux q_r in y -direction is given by [Brewster (1992)]

$$q_r = -\frac{4\sigma_s}{3k_e} \frac{\partial T^4}{\partial y}, \quad (9)$$

where σ_s is the Stefan-Boltzmann constant and k_e the mean absorption coefficient. It should be noted that by using Rosseland approximation, the present study is limited to optically thick fluids.

Expanding T^4 in a Taylor series about T_∞ as:

$$T^4 = T_\infty^4 + 4T_\infty^3(T - T_\infty) + 6T_\infty^2(T - T_\infty)^2 + \dots$$

Neglecting higher-order terms beyond the first degree in $(T - T_\infty)$, we get

$$T^4 \cong 4T_\infty^3 T - 3T_\infty^4, \quad (10)$$

In view of the equations (9) and (10), the equation (6) becomes

$$u \frac{\partial T}{\partial x} + v \frac{\partial T}{\partial y} = \alpha \frac{\partial^2 T}{\partial y^2} + \frac{16\sigma_s T_\infty^3}{3k_e \rho C_p} \frac{\partial^2 T}{\partial y^2}, \quad (11)$$

Introduce a Stream function Ψ as follows

$$u = \frac{\partial \Psi}{\partial y}, \quad v = -\frac{\partial \Psi}{\partial x}. \quad (12)$$

The momentum, angular momentum and energy equations can be transformed into the corresponding ordinary differential equations by the following transformation:

$$\eta = \sqrt{\frac{a}{v}} y, \quad f(\eta) = \frac{\Psi}{x\sqrt{av}}, \quad p(\eta) = \frac{N}{ax\sqrt{\frac{a}{v}}},$$

$$\theta(\eta) = \frac{k(T-T_\infty)}{q_w} \sqrt{\frac{a}{v}}, \quad H_1 = H_0 \frac{ax}{v} h'(\eta),$$

$$H_2 = -H_0 \sqrt{\frac{a}{v}} h(\eta), \quad (13)$$

where η the independent dimensionless similarity variable. Thus u and v are given by $u = axf'(\eta)$, $v = -\sqrt{av}f(\eta)$. Substituting variables (13) into equations (2) to (6), we get the following ordinary differential equations:

$$(1+K)f'''' + ff'' + 1 - f'^2 + Kp' + M(h'^2 - h h'' - 1) + \lambda\theta = 0, \quad (14)$$

$$\alpha_2 h'''' + f h'' - h f'' = 0, \quad (15)$$

$$\left(1 + \frac{K}{2}\right) p'' + fp' - pf' - K(2p + f') = 0, \quad (16)$$

$$\frac{1}{Pr} \left(1 + \frac{4}{3F}\right) \theta'' + f\theta' - \theta f' = 0, \quad (17)$$

subject to the boundary conditions (7) and (8) which become

$$f(0) = s, \quad f'(0) = e, \quad p(0) = -nf''(0), \\ \theta'(0) = -1, \quad h(0) = h''(0) = 0, \\ \text{as } \eta \rightarrow \infty: f'(\eta) \rightarrow 1, \quad p(\eta) \rightarrow 0$$

$$\theta(\eta) \rightarrow 0, \quad h'(\eta) \rightarrow 1. \quad (18)$$

Here $f'(\eta)$, $p(\eta)$, $h'(\eta)$ and $\theta(\eta)$ give (dimensionless) the velocity, the angular velocity, the induced magnetic field and temperature respectively. In the above equations, primes denote differentiation with respect to η ; $j = \frac{v}{a}$ the characteristic length [Rees & Bassom (1996)], $Pr = \frac{v}{\alpha}$ the Prandtl number, $M = \frac{\mu_e H_0^2}{\rho v^2}$ the magnetic parameter or Hartmann number, $\alpha_2 = \frac{\alpha_1}{v}$ is the reciprocal of the magnetic Prandtl number, $e=c/a$ the velocity ratio parameter, $s = -\frac{v_w(x)}{\sqrt{av}}$ the constant mass flux with $s>0$ for suction and $s<0$ for injection, $\lambda = \frac{Gr_x}{Re_x^{5/2}}$ the Buoyancy or mixed convection parameter, $F = \frac{k_e k}{4\sigma_s T_\infty^3}$ the radiation parameter, $Gr_x = \frac{g\beta(T_w - T_\infty)x^3}{\nu^2}$ the local Grashof number and $Re_x = \frac{Ux}{\nu}$ is the local Reynolds number. Here λ is a constant and the negative and positive values of λ correspond to the opposing and assisting flows respectively. When $\lambda=0$, i.e., when $T_w=T_\infty$ is for pure forced convection flow. Ramchandran et al (1988) considered the present problem with $M=0$ and $K=0$.

The skin friction coefficient C_f and the local Nusselt number Nu_x are defined as

$$C_f = \frac{\tau_w}{\rho U^2/2}, \quad Nu_x = \frac{xq_w}{k(T_w - T_\infty)}, \quad (19)$$

where the wall shear stress τ_w and the heat flux q_w are given by

$$\tau_w = \left[(\mu + \kappa) \frac{\partial u}{\partial y} + \kappa N \right]_{y=0},$$

$$q_w = -k \left[\frac{\partial T}{\partial y} \right]_{y=0}, \quad (20)$$

with k being the thermal conductivity. Using the similarity variables (10), we get

$$\frac{1}{2} C_f Re_x^{1/2} = \left[1 + (1-n) \frac{K}{2} \right] f''(0),$$

$$\frac{Nu_x}{Re_x^{1/2}} = \frac{1}{\theta(0)}. \quad (21)$$

3. Numerical Solutions:

The equations (14) – (17) subject to the boundary conditions (18) are solved numerically using an implicit finite-difference scheme known as the Keller-box method [Cebeci & Bradshaw (1988)]. The method has following four basic steps:

- i) Reduce Equations (14)-(17) to first order equations;
- ii) Write the difference equations using central differences;
- iii) Linearise the resulting algebraic equations by Newton's method and write them in Matrix-vector form;
- iv) Use the Block-tridiagonal elimination technique to solve the linear system.

The details are also described by Adhikari and Sanyal (2013).

4. Results & Discussion:

The step size $\Delta\eta$ of η and the edge of the boundary layer η_∞ had to be adjusted for different values of parameters to maintain accuracy within the interval $0 \leq \eta \leq \eta_\infty$, where η_∞ is the boundary layer thickness, we run the programme in MATLAB upto the desired level of accuracy. The validity of the numerical results has been compared with the results of Bachok and Ishak (2009) and they are found to be in a very good agreement, as presented in Table 1.

Table1: Values of $f''(0)$ and $1/\theta(0)$ for different values of P_r

(when $\lambda=1, K=0, n=0.5, M=0, \Delta\eta=0.02$)

P_r	Bachok & Ishak(2009)		Present result (for $s=0, e=0, n=0$)	
	$f''(0)$	$1/\theta(0)$	$f''(0)$	$1/\theta(0)$
0.7	1.8339	0.7776	1.8339	0.7776
1.0	1.7338	0.8781	1.7339	0.8781
7.0	1.4037	1.6913	1.4037	1.6913
10.0	1.3711	1.9067	1.3712	1.9072

The velocity, induced magnetic field, angular velocity and temperature distribution are given in the figures 1 to 17 for different parameters. Figures 1 and 5 respectively depict that the velocity profiles for the assisting flow decrease with the increase of M, P_r, K and F ; whereas for the opposing flow the velocity profiles decrease with M , increase with P_r and F but almost no change with K . With the increase of s , figure 6 describes that the velocity profiles for the assisting flow enhance near boundary and after $\eta=1$ it reduce, but for the opposing flow the velocity profiles increase. For the both flows velocity profiles raise with α_2 (fig.7). Figures 8 to 12 illustrate that the induced magnetic field distribution for the assisting flow boost with M, P_r, K, F and s ; but for the opposing flow it decrease with M , increase with P_r and s , almost no change with K and increase very slowly with F . Angular velocity profiles increase for the both flows with s and M (figs. 13 and 14). Temperature distribution for the both flows increase with M (fig 15), decrease with F and P_r (figs.16 and 17). Figures 18 and 19 represent that the Skin friction coefficient and the local Nusselt number decrease with M for the both flows.

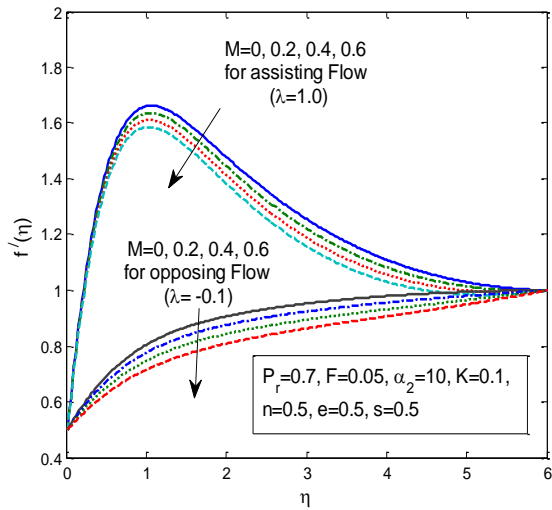


Fig.2 : Velocity distribution for different M

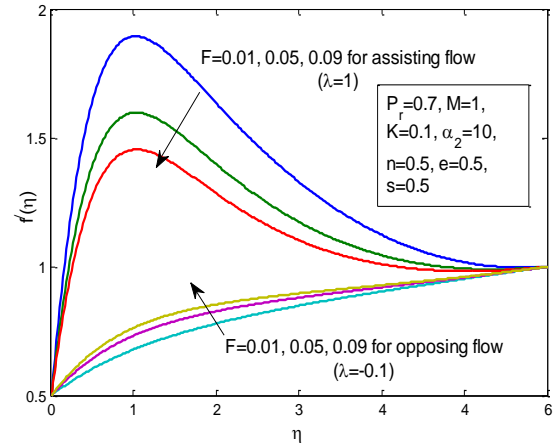


Fig.5: Velocity Distribution for different F

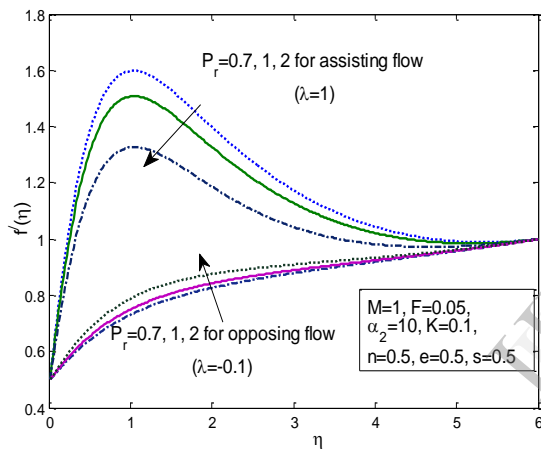


Fig.3 Velocity distribution for different P_r

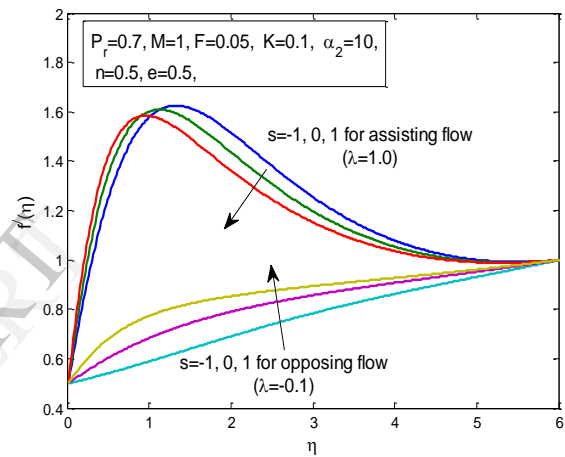


Fig.6: Velocity distribution for different s

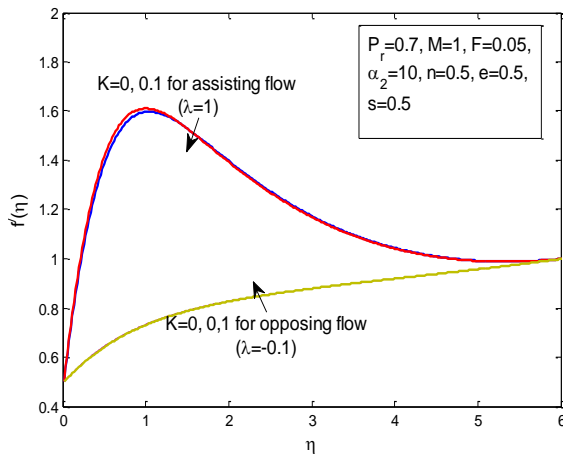


Fig.4: Velocity distribution for different K

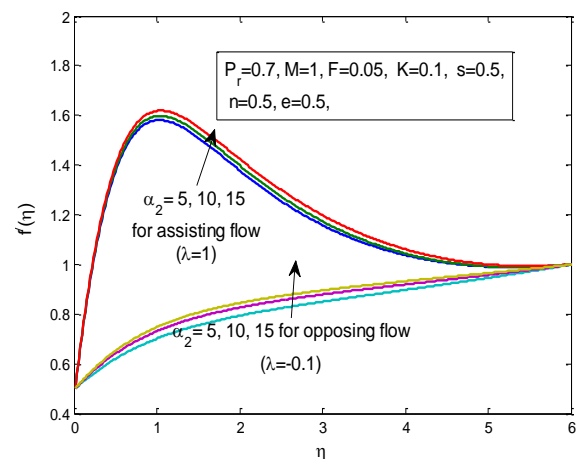


Fig.7: velocity distribution for different α_2

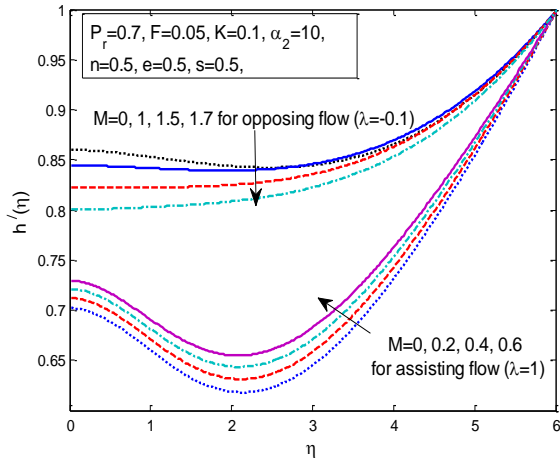


Fig.8: Induced magnetic field for different M

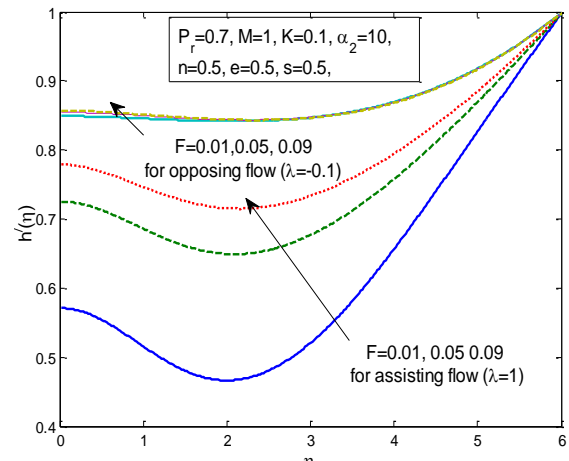


Fig 11: Induced Magnetic field for different F

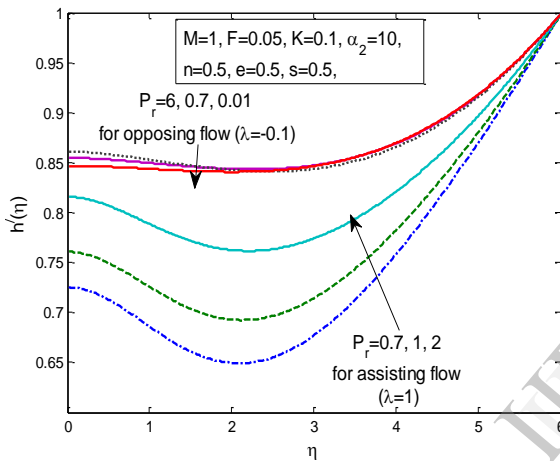


Fig 9: Induced Magnetic field for different P_r

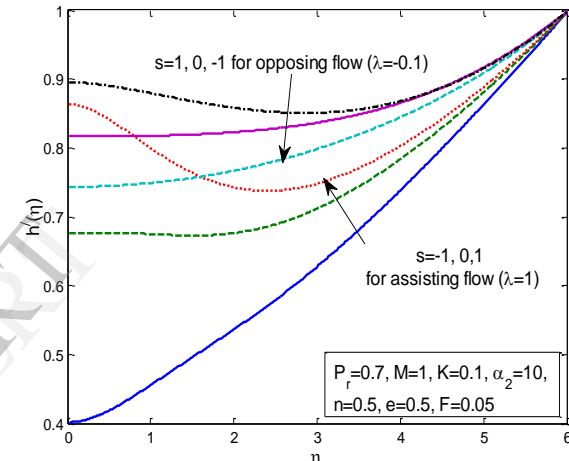


Fig.12: Induced magnetic field for different s

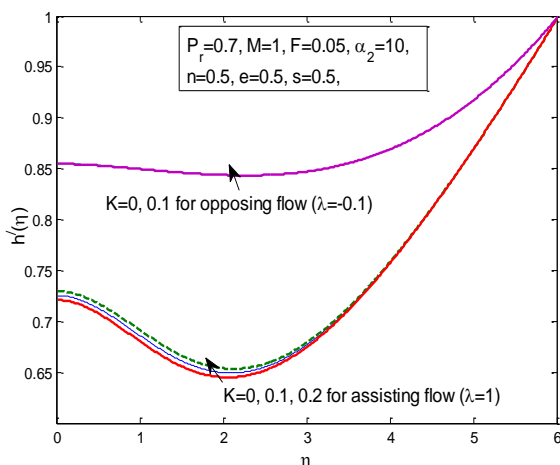


Fig 10: Induced Magnetic field for different K

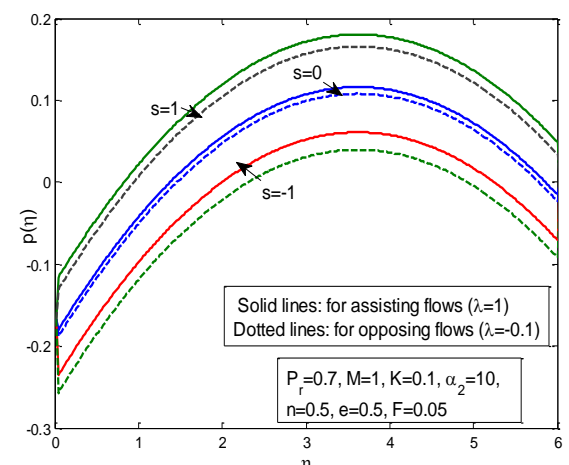


Fig 13: Angular velocity for different s

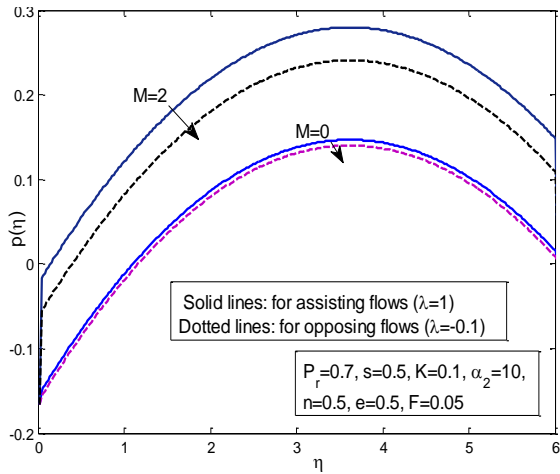


fig 14: Angular velocity for different M

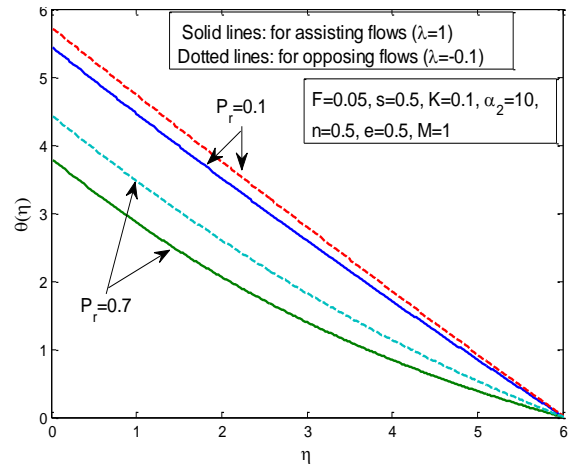


Fig 17: Temperature distribution for different P_r

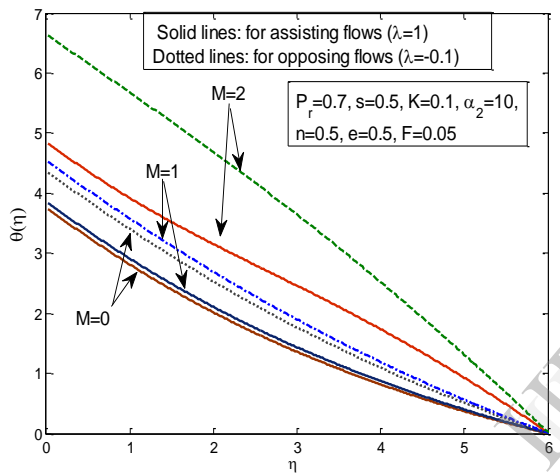


Fig.15: Temperature distribution for different M

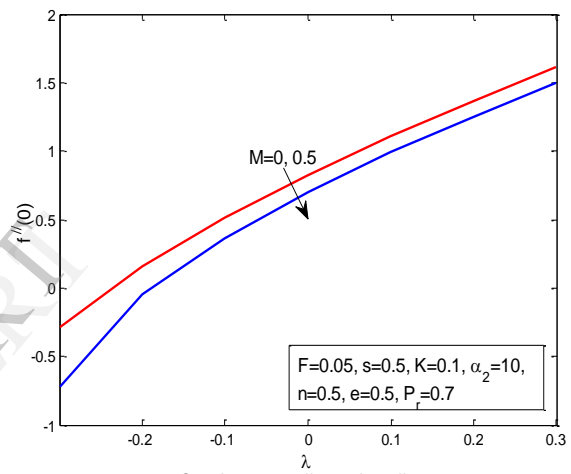


Fig18: Skin friction coefficient for different M

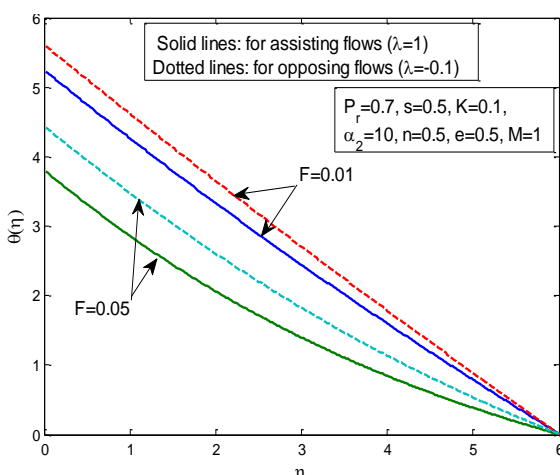


Fig 16: Temperature distribution for different F

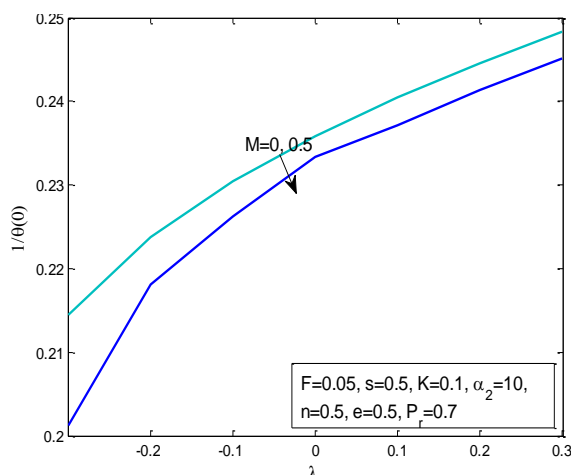


Fig. 19: Local Nusselt number for different M

Acknowledgement:

The author gratefully acknowledges the financial support received from the UGC, India (Minor Research Project: PSW 145/11-12 (ERO) 25 Jan 12).

References:

- [1]. Adhikari A. and Sanyal D.C., "Heat transfer on MHD viscous flow over a stretching sheet with prescribed heat flux", *Bull. Int. Math. Virtual Instt.*, **3**, (2013), 35-47.
- [2]. Ahmadi G., "Self-similar solution of incompressible micropolar boundary layer flow over a semi-infinite flat plate", *Int. Jr. Engg. Sci.*, Vol. 14, (1976), pp 639-646.
- [3]. Ali F.M., Nazar R., Arifin N.M. and Pop I., "MHD Mixed Convection Boundary Layer Flow Towards a Stagnation Point on a Vertical Surface with Induced Magnetic Field", *Jr. of Heat Transfer*, Vol. **133**, (2011), pp 022502 1-6
- [4]. Ariman T., Turk M.A. and Sylvester N.D., "Microcontinuum fluid mechanics- review", *Int. Jr. Engg. Sci.*, Vol. 11, (1973), pp 905-930.
- [5]. Ariman T., Turk M.A. and Sylvester N.D., "Application of Microcontinuum fluid mechanics", *Int. Jr. Engg. Sci.*, Vol.12, (1974), pp 273-293.
- [6]. Bachok N. and Ishak A., "MHD stagnation-point flow of a Micropolar Fluid with Prescribed Wall Heat Flux", *European Jr. of Sci. Research*, Vol.-35, No.-3, (2009), pp 436-443.
- [7]. Brewster, M.Q., *Thermal Radiative Transfer Properties*, John Wiley and Sons, Canada, 1992.
- [8]. Cebeci T. and Bradshaw P., "Physical and Computational Aspects Convective Heat Transfer", 1988, Springer, New York.
- [9]. Chin K.E., Nazar R., Arifin N. and Pop I., "Effect of variable viscosity on mixed convection boundary layer flow over a vertical surface embedded in a porous medium", *Int. Comm. Heat Mass Transf.*, Vol. 34, (2007), pp 464-473.
- [10]. Das K., "Hydromagnetic thermal boundary layer flow of a perfectly conducting fluid", *Turk Jr. Phy.*, 35 (2011), 161-171.
- [11]. Devi C.D.S., Takhar H.S., and Nath G., "Unsteady mixed convection flow in stagnation region adjacent to a vertical surface", *Heat Mass Transfer*, Vol. 26, (1991), pp 71-79.
- [12]. Eringen A.C., "Theory of Micropolar Fluids", *Jr. Math. Mech.*, Vol.16, (1966), pp 1-18.
- [13]. Eringen A.C., "Theory of Thermomicropolar Fluids", *Jr. Math. Appl.*, Vol.38, (1972), pp 480-495.
- [14]. Eringen A.C., "Microcontinuum field theories, II. Fluent Media". 2001, Springer, New York.
- [15]. Ishak A., Nazar R. and Pop I., "Magnetohydrodynamic stagnation point flow towards a stretching vertical sheet in a micropolar fluid", *Magnetohydrodynamic* 43, (2007), pp 83-97.
- [16]. Ishak A., Nazar R. and Pop I., 2008, "Mixed convection stagnation point flow of a micropolar fluid towards a stretching sheet", *Mechanica* 43, pp 411-418.
- [17]. Kumari, M., Takhar, H.S., and Nath, G., "MHD Flow and Heat Transfer Over a Stretching Surface With Prescribed Wall Temperature or

- Heat Flux”, *Waerme- Stoffuebertrag*, **25**, (1990), pp 331-336.
- [18]. Ling S.C., Nazar R. and Pop I., “Steady mixed convection boundary layer flow over a vertical flat plate in a porous medium filled with water at 4⁰C: case of variable wall emperature”, *Trans. Porous Med.*, **69**, (2007), pp 359-372.
- [19]. Lok Y. Y., Amin N., Campean D. and Pop I., “Steady mixed convection flow of a micropolar fluid near the stagnation point on a vertical surface”, *Int. Jr. Num. Methods Heat Fluid Flow*, **15**, (2005), pp 654-670.
- [20]. Lukaszewicz G., “*Micropolar fluids: theory and application*”, 1999, Birkhäuser, Basel.
- [21]. Mukhopadhyay S., Uddin S. and Layek G.C., “Lie group analysis of MHD boundary layer slip flow past a heated stretching sheet in presence of Heat source/sink”, *Int. Jr. Appl. Math. & Mech.*, **8**(16), (2012), 51-66.
- [22]. Ramachandran N., Chen T.S. and Armaly B.F., “Mixed convection in stagnation flows adjacent to a vertical surfaces”, *ASME Jr. Heat Transfer*, **110**, (1988), pp 373-377.
- [23]. Raptis, A. and Perdikis, C., “Free Convection Under the Influence of a Magnetic Field”, *Nonlinear Anal. Theory, Methods Appl.*, **8**, (1984), pp 749-756.
- [24]. Rees D.A.S. and Bassom A.P., “The Blasius boundary-layer flow of a micropolar fluid”, *Int. Jr. Engg. Sci.* **34**, (1996), pp 113-124.
- [25]. Shit G.C. and Halder R., “Thermal radiation effects on MHD viscoelastic fluid flow over a stretching sheet with variable viscosity”, *Int. Jr. of Appl. Math. & Mech.*, **8**(14), (2012), 14-36.
- [26]. Takhar, H.S., Kumari, M., and Nath, G., “Unsteady Free Convection Flow Under the Influence of a Magnetic Field”, *Arch. Appl. Mech.*, **63**, (1993), pp.313-321.
- [27]. Yücel A., “Mixed convection in micropolar fluid flow over a horizontal plate with surface mass transfer”, *Int. Jr. Engg. Sci.*, **27**, (1989), pp 1593-1602.